Available online at www.sciencedirect.com

ScienceDirect

Procedia Engineering 81 (2014) 1348 – 1353

Procedia Engineering

www.elsevier.com/locate/procedia

11th International Conference on Technology of Plasticity, ICTP 2014, 19-24 October 2014, Nagoya Congress Center, Nagoya, Japan

Application of a gradient crystal plasticity model to numerical analysis of metal part of nanoporous metal – polymer composites

Natalia Konchakova[a,]*, Swantje Bargmann[a,b]

[a]*Hamburg University of Technology, Institute of Continuum Mechanics and Material Mechanics, Eißendorfer Str. 42, 21073 Hamburg, Germany*

[b]*Institute of Materials Research, Helmholtz-Zentrum Geesthacht, Max-Planck-Str. 1, 21502 Geesthacht, Germany*

Abstract

The application of a gradient extended theory to the computation of the mechanical response of a single crystalline sub-micron gold, which is the part of nano-composites, is in the focus of the contribution. The research takes into account the dependence of the macroscopic behavior of a crystalline material on the size and morphology of the grains, the volume fraction of different phases, and the subgrain material modeling. A gradient hardening contribution is included into the crystal plasticity model in order to study the influence of the grain size on the response of single crystalline. It is assumed that the grain boundaries act as barriers to plastic deformation. The highly coupled system of equations is solved by applying a dual mixed finite element algorithm. Numerical results of the sub-micron gold crystal deformation under cyclic shear loading are presented. The gradient effect in the deformation field is discussed.

Selection and peer-review under responsibility of the Department of Materials Science and Engineering, Nagoya University

Keywords: Gradient hardening; Extended crystal plasticity; Sub-micron gold; Finite elements; Size effect

* Corresponding author. Tel.: +49-40-428-78-3036; fax: +49-40-428-78-3428.
E-mail address: natalia.konchakova@tu-harburg.de

Selection and peer-review under responsibility of the Department of Materials Science and Engineering, Nagoya University
doi:10.1016/j.proeng.2014.10.155

1. Introduction

The focus of the research is the investigation of metal – polymer composites. The overarching significance is elucidated by the mechanical characterization of these material structures. In this contribution the numerical analysis of the composite's metal part - in our case nanoporous gold - is considered. This material system is very attractive for sensor applications, for example. Further, the use of nanoporous gold in composites allows for the development of advanced materials, such as low-density high-strength foams, as well as high-surface low-elastic modulus coatings for chemo-mechanical sensors, see, e.g., Seker et al. (2009). Nanoporous gold has intriguing material properties that show potential benefits for some applications due to its high specific surface area, high electrical conductivity, and reduced stiffness. The experimental investigations show a significant size effect in nano deformations of nanoporous gold (Greer et al. (2005); Volkert and Lilleodden (2006)).

Simulations and numerical analysis of the experimentally observed phenomena, especially the size effect, can be realized by application of a gradient extended crystal plasticity theory, see, e.g., Gurtin (2000), Evers et al. (2004), Bardella (2006), Ohno and Okumura (2007), Kuroda and Tvergaard (2008), Lele and Anand (2008), Svendsen and Bargmann (2010), Bargmann and Ekh (2013). The model applied in the current contribution is based on Bargmann et al. (2011). The single crystal gold is considered as a basic part of a nano-porous gold structure.

2. Material modeling

In this work, the study of the mechanical behavior of nanoporous gold is done within the framework of extended continuum mechanics. Single crystal gold is considered as a part of a solid body undergoing a nanodeformation. From this point of view, the crystal reflects the physical properties of the solid body B. The crystal deforms continuously under the action of applied forces, displacements and tractions. The body B in the undeformed and stress-free configuration B_0 is homogeneous and does not have any singularities. The kinematics are based on the multiplicative split of the deformation gradient $\mathbf{F}$ into an elastic $\mathbf{F}_\mathrm{e}$ and a plastic part $\mathbf{F}_\mathrm{p}$ which dates back to Lee (1969) and Rice (1971):

$$\mathbf{F} = \mathbf{F}_\mathrm{e} \cdot \mathbf{F}_\mathrm{p} . \tag{1}$$

The deformation is studied with help of the right Cauchy-Green tensor $\mathbf{C}$ in the reference configuration

$$\mathbf{C} = \mathbf{F}_\mathrm{p}^\mathrm{T} \cdot \overline{\mathbf{C}}_\mathrm{e} \cdot \mathbf{F}_\mathrm{e} , \tag{2}$$

the elastic right Cauchy-Green tensor $\overline{\mathbf{C}}_\mathrm{e} = \mathbf{F}_\mathrm{e}^\mathrm{T} \cdot \mathbf{F}_\mathrm{e}$ in the intermediate configuration $\overline{B}$ and the elastic Green-Lagrange strain

$$\overline{\mathbf{E}}_\mathrm{e} = \frac{1}{2}\left[\mathbf{C}_\mathrm{e} - \mathbf{I}\right], \tag{3}$$

in the intermediate configuration $\overline{B}$. The relevant stress measures are the first Piola-Kirchhoff stress $\mathbf{P}$

$$\mathbf{P} = \mathbf{F}_\mathrm{e} \cdot \overline{\mathbf{S}}_\mathrm{e} \cdot \left[\mathbf{F}_\mathrm{p}^{-1}\right]^\mathrm{T}, \tag{4}$$

and the second Piola--Kirchhoff stress $\overline{\mathbf{S}}_\mathrm{e}$

$$\overline{\mathbf{S}}_\mathrm{e} = \mathbf{F}_\mathrm{e}^{-1} \cdot \tau \cdot \left[\mathbf{F}_\mathrm{e}^{-1}\right]^\mathrm{T} . \tag{5}$$

Here, τ is the Kirchhoff stress. The deformation problem is linked to the microscopic behavior via the plastic velocity gradient tensor $\overline{\mathbf{L}}_\mathrm{p}$:

$$\overline{\mathbf{L}}_\mathrm{p} = \dot{\mathbf{F}}_\mathrm{p} \cdot \mathbf{F}_\mathrm{p}^{-1} = \sum_\alpha \nu_\alpha \left[\overline{\mathbf{s}}_\alpha \otimes \overline{\mathbf{n}}_\alpha\right], \tag{6}$$

where the slip rate ν_α, the slip direction $\overline{\mathbf{s}}_\alpha$ and slip normal $\overline{\mathbf{n}}_\alpha$ are introduced. Together with the direction $\overline{\mathbf{t}}_\alpha = \overline{\mathbf{n}}_\alpha \times \overline{\mathbf{s}}_\alpha$ they form an orthonormal system on the slip system α. The resolved shear stress is associated with the slip system and defined as

$$\tau_\alpha = \overline{\mathbf{s}}_\alpha \cdot \overline{\mathbf{M}}_\mathrm{e} \cdot \overline{\mathbf{n}}_\alpha , \tag{7}$$

where $\overline{\mathbf{M}}_{\mathrm{e}} = \overline{\mathbf{C}}_{\mathrm{e}} \cdot \overline{\mathbf{S}}_{\mathrm{e}}$ is the Mandel stress on the intermediate configuration $\overline{B}$. The mechanical problem is governed by the balance of momentum

$$\mathbf{0} = \mathrm{Div}\,\mathbf{P} + \mathbf{b}_0, \tag{8}$$

where $\mathbf{b}_0$ is the body force.
Further, the free energy $\overline{\Psi}$ is introduced as a function of the elastic right Cauchy-Green deformation tensor $\overline{\mathbf{C}}_{\mathrm{e}}$, the plastic slip rate ν_α and the slip rate gradient $\nabla_{\mathrm{i}}\nu_\alpha$:

$$\overline{\Psi} = \overline{\Psi}\left(\overline{\mathbf{C}}_{\mathrm{e}}, \nu_\alpha, \nabla_{\mathrm{i}}\nu_\alpha\right) \tag{9}$$

(here and below the index " i " refers to the intermediate configuration). Thus, the free energy includes gradient effects. In the following, model properties are introduced for the description of the effect of geometrically necessary dislocations (GNDs), size dependent hardening behavior as well as the Bauschinger effect. In our case, the free energy is split into an elastic and two hardening parts:

$$\overline{\Psi}\left(\overline{\mathbf{C}}_{\mathrm{e}}, \nu_\alpha, \nabla_{\mathrm{i}}\nu_\alpha\right) = \overline{\Psi}_{\mathrm{e}}\left(\overline{\mathbf{C}}_{\mathrm{e}}\right) + \overline{\Psi}_{\mathrm{ln}}\left(\nu_\alpha\right) + \overline{\Psi}_{\mathrm{gh}}\left(\nabla_{\mathrm{i}}\nu_\alpha\right), \tag{10}$$

where $\overline{\Psi}_{\mathrm{e}}\left(\overline{\mathbf{C}}_{\mathrm{e}}\right)$ is the elastic contribution. The hardening contribution is decomposed into local hardening $\overline{\Psi}_{\mathrm{ln}}\left(\nu_\alpha\right)$ and gradient hardening $\overline{\Psi}_{\mathrm{gh}}\left(\nabla_{\mathrm{i}}\nu_\alpha\right)$:

$$\frac{\partial \dot{\overline{\Psi}}_{\mathrm{lh}}}{\partial \nu_\alpha} = \sum_\beta H^l_{\alpha\beta}\,\nu_\beta, \qquad \overline{\Psi}_{\mathrm{gh}} = \frac{1}{2} l^2 H^g \sum_{\alpha,\beta} \left[\mathbf{b}_\alpha \cdot \mathbf{b}_\beta\right] g_{\mathrm{i}\alpha}\, g_{\mathrm{i}\beta}$$

Here, the local hardening modulus $H^{\mathrm{l}}_{\alpha\beta}$ and the gradient hardening modulus H^{g} are introduced. Further, b is the length of the Burgers vector $\mathbf{b}_\alpha = b\,\overline{\mathbf{s}}_\alpha$, and l is an internal length. Following Bargmann et al. (2011), we introduce the following evolution equations for the geometrically necessary dislocations (GND) densities g_{i}

$$\dot{g}_{\mathrm{i}\alpha} = \sum_\beta \nu_\alpha \left[\overline{\mathbf{n}}_\alpha \cdot \overline{\mathbf{s}}_\beta\right] g_{\mathrm{i}\beta} + \frac{1}{b} \nabla_{\mathrm{i}}\nu_\alpha \cdot \overline{\mathrm{s}}_\alpha\,. \tag{11}$$

The first term captures latent hardening, while the second term maps size effects. Moreover, following Ekh et al. (2007), we introduce a hardening microstress κ_α

$$\dot{\kappa}_\alpha = \frac{\partial \dot{\overline{\Psi}}_{\mathrm{i}}}{\partial \nu_\alpha} - \mathrm{Div}_{\mathrm{i}}\left(\frac{\partial \dot{\overline{\Psi}}_{\mathrm{i}}}{\partial \nabla_{\mathrm{i}}\nu_\alpha}\right). \tag{12}$$

The elastic response E is described as

$$E = \left\{\tau \,\middle|\, \Phi_\alpha\left(\tau_\alpha, \kappa_\alpha\right) \le 0,\ \alpha = 1, 2, \ldots, n_{\mathrm{slip}}\right\},$$

where $\Phi_\alpha = \tau_\alpha - \left[Y_\alpha + \kappa_\alpha\right]$ is the yield function. The initial yield stress Y_α and the hardening microstress κ_α characterize the material behavior in the plastic state. The flow rule is assumed as follows

$$\nu_\alpha = \frac{1}{t_*}\left[\frac{\langle \Phi_\alpha \rangle}{C_0}\right]^m. \tag{13}$$

The relaxation time t_*, the constant drag stress C_0 and the rate sensitivity parameter m are the same for all slip systems.

3. Numerical examples

3.1. Finite element formulation and discretization

For solving the highly coupled and nonlinear system of governing equations a so-called dual mixed finite element algorithm is used, cf. Ekh et al. (2007), Svedberg and Runesson (1998). The finite element method in space and a mixed implicit-explicit integration procedure in time are realized. A monolithic Newton-Raphson iteration scheme is used to account for the coupling resp. the nonlinearity of the equations. The finite element mesh

consist of 1226 elements and 1297 nodes. Six slip systems are assumed for the face central cubic (FCC) crystal. For the plastic slip rate, micro-hard conditions are assumed on the boundary:

$$\nu_\alpha = 0 \text{ on } \partial B_0 . \tag{14}$$

Boundary conditions for the mechanical problem are given by prescribing the displacements at the boundaries of the crystal structure. Plane strain conditions are assumed. Computations are carried out for the cyclic loading during which simple shear deformation to the right is applied first. Then, the load is reversed and the crystal is simple-shear-deformed to the left afterwards. Simulations of three loading cycles in monotonic loading are run. Different side lengths L of the crystal structure are analyzed.

3.2. Sub-micron single crystal gold

Single crystal sub-micron gold is under consideration. The mechanical behavior of the gold is investigated in the experiments of, e.g., Volkert and Lilleodden (2006), Jin et al. (2009), Seker et al. (2009). As observed in tests, the strength of nanoporous gold crystals increases when the crystal dimensions are reduced. Taking the experimental data as a basis, the grain lengths L of 1, 10 and 22 μm are used in the numerical tests to investigate the size effect. The Young`s modulus of 79 GPa, Poisson`s ratio of 0.44, the yield stress of nanoporous gold of 154 MPa, and the strain hardening coefficient of 472 MPa are stated in Volkert and Lilleodden (2006).

The macro-scale cyclic loading with the maximal strain magnitude of 0.025 to the right and to the left direction for different lengths of sub-micron gold crystal structure are simulated. Monotonic loading with the constant loading rate is accomplished. 240 equidistant time steps are applied. Three loading cycles are simulated. The numerical results are presented in Figures 1-3.

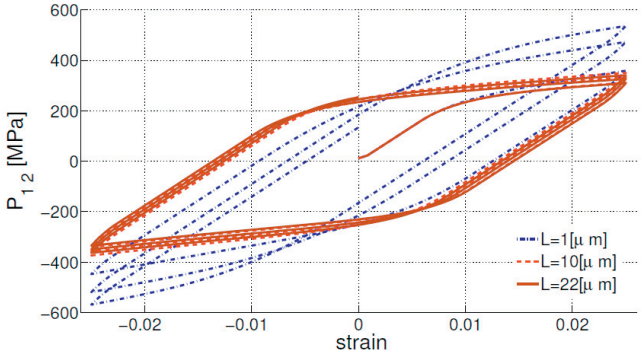

Fig. 1. Macroscopic stress-strain response for cycling loading of single crystalline gold.

The macroscopic stress-strain response in terms of the nominal shear stress component versus the macroscopic strain is shown in Fig. 1 for the crystal side lengths L of 1, 10 and 22 μm. The stress-strain responses show the strong size effect which is caputred due to the existence of the gradient hardening part in the evolution equation of the GND density. Moreover, the Bauschinger effect is clearly observed. The yield stress decreases after the loading direction is reversed. It can be explained by the motion of the dislocations. Upon load reversal, the local back stress allows the dislocations to move easily in the reverse direction, resulting in a lower yield stress. The points of maximal loading on each loading cycle are different for all three cases. The difference between the extreme stress values increases with decreasing crystal dimensions. The numerical results demonstrate the strong size dependence of the maximal stress values with fixed material parameters and given strain. Moreover, the phenomena of the increasing hardening due to plastic deformation during each loading cycles can be observed for all three macroscopic stress-strain curves.

Local obstacles to dislocation motion, e.g., at grain boundaries, lead to geometrically necessary dislocations. The increase in hardening in the second and third cycle is quite intensive for the crystal with the smallest grain size compared to the other crystals under consideration. The difference of the increasing hardening on the same loading cycles for the crystals with the side length L of 10 and 22 μm are rather small. Thus, a stiffer mechanical response

in the hardening regime is seen for smaller crystal sizes. It demonstrates once more the dependence on the microstructural length.

To study the hardening nature, the distributions of the effective hardening and the effective geometrically necessary dislocations density after the third cycle for a grain structure with grain length L = 1 μm are depicted in Figs. 2 and 3.

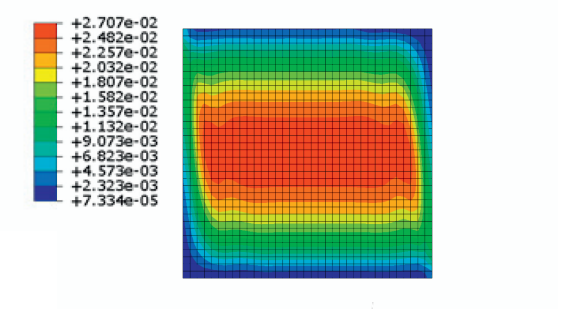

Fig. 2. Distribution of effective hardening $\left(\sqrt{\sum_{\alpha} \left(\int_{t} v_{\alpha} \, dt \right)^{2}} \right)$.

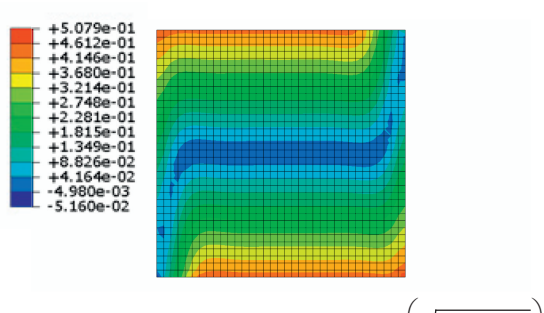

Fig. 3. Distribution of effective GND density $\left(\sqrt{\sum_{\alpha} \left(g_{i\alpha} \right)^{2}} \right)$.

In the end of the loading the hardening is more active in the central area of the crystal and it is vanishes near the crystal boundaries which mimics the assumed micro-hard boundary conditions (see Fig. 2). The analysis of the geometrically necessary dislocations density (Fig. 3) shows that the extreme values are placed at the boundaries of the crystal. The distribution indicates that dislocations move more intensively at the horizontal crystal boundaries due to the shear cycling loading in the same direction. The dislocations act stronger at the crystal walls and vanish towards the structure`s core.

4. Discussion and Conclusion

The gradient extended crystal plasticity model has been applied to the computation of the mechanical response of metal part of singe crystalline gold. The size length L of the grain was varied during the simulations in order to study its influence. The mechanical behavior of the nanoporous gold crystals with the side lengths of 1, 10 and 22 μm are modeled for the case of cyclic shear loading. The introduction of the gradient hardening part allows to describe the grain size dependent plastic deformation and the Bauschinger effect. This is in accordance to the experimental results on the strength investigation in nanoporous gold (Wang and Weissmüller, 2013). The strength of crystals is increased when the crystal dimensions are reduced. Moreover, the changes of the maximal values of stresses in each load cycle are seen. The crystal with the smaller grain size has the stronger difference between the extreme stress values. The dependence of the hardening rate on the grain size is observed. The stiffer hardening response can be observed for smaller grain size. It corresponds to the experimental data on the investigation of size effects in the deformation of sub-micron Au columns in which the strain hardening rate increases strongly with decreasing column diameter (Volkert and Lilleodden, 2006).

The model applied in the current work allows to describe latent hardening, i.e., the hardening of inactive slip systems due to active slip systems. Six active slip systems are assumed in the simulation of face central cubic crystal of nanoporous gold. The active and latent states of the slip system are accounted for during calculation. Of course, if one or more glide systems are latent, it does not mean that the plastic deformation is absent in the material (see Eq. (11)).

Acknowledgements

The authors gratefully acknowledge financial support from the German Research Foundation (DFG) via SFB 986 "M^3", project B6.

References

Balint, D.S., Deshpande, V.S., Needleman, A., 2005. A discrete dislocation plasticity analysis of grain-size strengthening. Materials Science and Engineering: A 400-401, 186-190.

Bardella, L., 2006. A deformation theory of strain gradient crystal plasticity that account for geometrically necessary dislocations. Journal of the Mechanics and Physics of Solids, 54, 128-160.

Bargmann, S., Ekh, M., Runesson, B. and Svendsen, B., 2010. Modeling of polycrystals with gradient crystal plasticity a comparison of strategies. Philosophical Magazine, 90(10), 1263-1271.

Bargmann, S., Svendsen, B. and Ekh, M., 2011. An extended crystal plasticity model for latent hardening in polycrystals. Computational Mechanics, 48, 631-645.

Bargmann, S. and Ekh, M., 2013. Microscopic temperature field prediction during adiabatic loading in a gradient extended crystal plasticity theory. International Journal of Solids and Structures, 50, 899-908.

Greer, J. R., Oliver, W.C. and Nix, W. D., 2005. Size dependence of mechanical properties of gold at the micron scale in the absence of strain gradients. Acta Materialia, 53(6), 1821-1830.

Gurtin, M., 2000. On the plasticity of single crystals: free energy, microforces, plastic-strain gradient. Journal of the Mechanics and Physics of Solids, 48, 989-1036.

Gurtin, M., 2008. A theory of grain boundaries that accounts automatically for grain misorientation and grain-boundary orientation. Journal of the Mechanics and Physics of Solids, 56 (2), 640-662.

Ekh, M., Grymer, M., Runesson, K. and Svedberg, T., 2007. Gradient crystal plasticity as part of the computational modelling of polycrystals. International Journal for Numerical Methods in Engineering, 72, 197-220.

Evers, L.P., Brekelmans, W.A.M. and Geers, M.G.D., 2004. Non-local crystal plasticity model with intrinsic SSD and GND effects. Journal of the Mechanics and Physics of Solids, 52, 2379 –2401.

Jin, H. J., Kurmanaeva, L., Schmauch, J., Rösner, H., Ivanisenko, Y. and Weissmüller, J., 2009. Deforming nanoporous metal: Role of lattice coherency. Acta Mater., 57, 2665-2672.

Kuroda, M. and Tvergaard, V., 2008. On the formulations of higher-order strain gradient crystal plasticity models. Journal of the Mechanics and Physics of Solids, 56, 1591 –1608.

Lee, E. H., 1969. Elastic-plastic deformation at finite strains. J. Appl Mech, 36, 1-6.

Lele, S. P. and Anand, L., 2008. A small-deformation strain-gradient theory for isotropic viscoplastic materials. Philosophical Magazine, 88, 3655–3689.

Nye J.F., 1953. Some geometric relations in dislocated crystals, Acta Metall, 1, 153-162.

Ohno, N., and Okumura, D., 2007. Higher-order stress and grain size effects due to self energy of geometrically necessary dislocations. Journal of the Mechanics and Physics of Solids, 55, 1879–1898

Rice, J., 1971. Inelastic constitutive relations for solids: an internal variable theory and its application to metal plasticity. J Mech Phys Solids, 19, 433–455.

Seker, E., Reed, M. L. and Berley, R., 2009. Nanoporous gold: Fabrication, Characterization, and Applications. Materials, 2, 2188-2209.

Svedberg, T. and Runesson, K., 1998. An algorithm for gradient-regularized plasticity coupled to damage based on a dual mixed FE-formulation, Comput. Methods Appl. Mech. Engrg., 16, 49-61.

Svendsen, B. and Bargmann, S., 2010, On the continuum thermodynamic rate variational formulation of models for extended crystal plasticity at large deformation, Journal of the Mechanics and Physics of Solids, 58, 1253- 1271.

Volkert, C. and Lilleodden, E., 2006. Size effect in the deformation of sub-micron Au columns. Philosophical Magazine, 86, 5567-5579.

Wang, K. and Weissmüller, J., 2013. Composites of nanoporous gold and polymer. Advanced Materials, 25, 1280-1284.